TARGET DESIGN FOR HALL TRANSMISSION SENSORS

By Dr. Dominik Weiland, Syed Bilal Ali, and Eric Burdette
Allegro MicroSystems

INTRODUCTION

Ferromagnetic targets come in all shapes and sizes. Depending on the type of application, the teeth can be of almost any form, including straight, stamped, spiral, or helical. Therefore, when designing a system with a magnetic sensor and ferromagnetic target, a common question is “what is the perfect target geometry?” In short, there is no perfect target geometry, and unless many of the free parameters that influence the magnetic interaction are specified, predicting performance for a set of gear geometries cannot be easily addressed.

However, it is possible to discuss the relative effects of varying one or two of the system parameters if the others are defined. In this application note, the magnet designs are fixed by using Allegro IC packages with integrated magnet and pole piece (concentrator). Specifically, two direction-detection transmission speed sensor ICs—the ATS692LSH and ATS19520LSN—are considered.

Both straight-toothed targets and stamped targets are considered, as shown in Table 1 and Table 2 respectively. Targets considered contain only features of uniform geometry.

Data and graphs will show some of the properties of the desired signal shape and amplitude when parameters such as tooth and valley width are varied. The information herein can be used as a general guide for coarsely predicting performance for a set of gear geometries; validation should always be done through applications analysis. For support, contact your local Allegro sales representative.

FREE DESIGN PARAMETERS

Multiple factors that influence Hall IC performance with a ferromagnetic target include:

- Tooth shape (i.e. rectangular or triangular, and radius of edge)
- Tooth arc length
- Valley arc width
- Tooth height
- Target face width (thickness)
- Properties of integrated magnet (shape, material)

Target Material

The magnetic permeability of the target material is not discussed in this application note. For that information, refer to application note *AN296132: Impact of Magnetic Relative Permeability of Ferromagnetic Target on Back-Biased Sensor Output*, available at allegromicro.com.

Table 1: Parameter definitions for Allegro Reference Target 60-0.

Parameter	Symbol	Nominal Value	Units	Symbol Key
Outer Diameter	D_o	120	mm	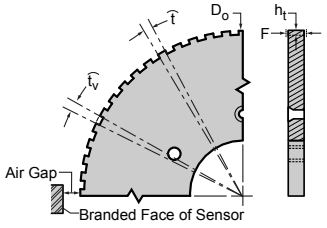
Target Thickness	F	6	mm	
Circular Tooth Length	t	3.14	mm	
		3	degrees	
Circular Valley Width	t_v	3.14	mm	
		3	degrees	
Tooth Height	h_t	3	mm	

Table 2: Parameter definitions for stamped target.

Parameter	Symbol	Nominal Value	Units	Symbol Key
Diameter	D	100	mm	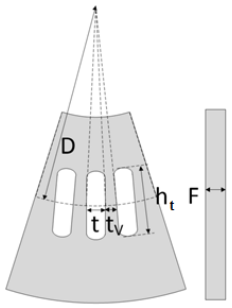
Target Thickness	F	3	mm	
Tooth Width	t	2.6	mm	
Valley Width	t_v	2.6	mm	
Tooth Height	h_t	3	mm	

SENSORS

Two of Allegro's transmission-specific sensors—ATS692LSH and ATS19520LSN—have been simulated, allowing for measurement of speed and direction of rotating targets.

Table 3: Details of sensors used in simulations

	ATS692LSH	ATS19520LSN
Hall-Element Spacing	1.75 mm	1.5 mm
Package Code	SH	SN

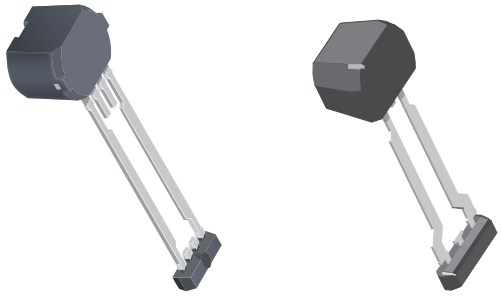

SH Package SN Package

Figure 1: Sensor IC packages used in the simulation

DATA

For each investigated parameter set, the differential magnetic signals sensed by the Hall IC were analyzed for a range of angular positions and air gaps. The sensors under discussion contain a total of three Hall elements oriented in a row, a back-biasing magnet, and a pole-piece to concentrate the field lines, as shown in Figure 2.

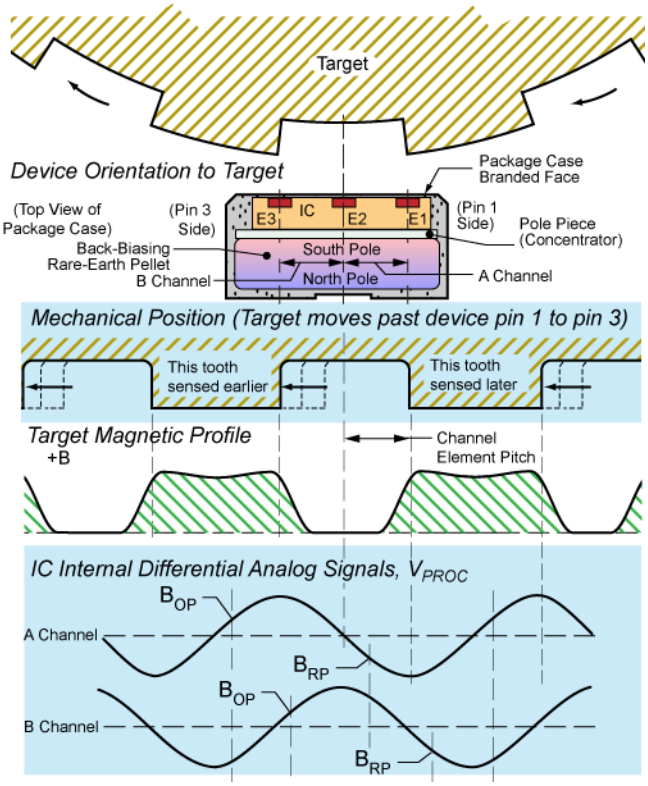

Figure 2: Definition of sensor channels.

From the three Hall elements, two differential channels are calculated by subtracting the magnetic field measured by E2 from the field measured by E3 and E1, respectively. These differential channels are called Channel A and Channel B. An example of this data is shown in Figure 3. Note that the Hall elements in the simulated devices are only sensitive to the component of the magnetic field that is normal to the face of the IC. To determine the maximum air gap for a given sensor/target combination, the signal amplitude at each air gap is extracted from the curves shown in Figure 3. These are plotted in Figure 4, and the method for determining minimum and maximum air gap is shown.

For direction detection ICs, a second critical parameter to evaluate is magnetic signal shape, in order that direction detection and vibration detection function properly under all conditions. This shape assessment is commonly distilled to a Switch Point Separation specification on the datasheet. At each switch point crossing, the vertical difference of the normalized magnetic channels (example shown in Figure 5) must meet a minimum criterion.

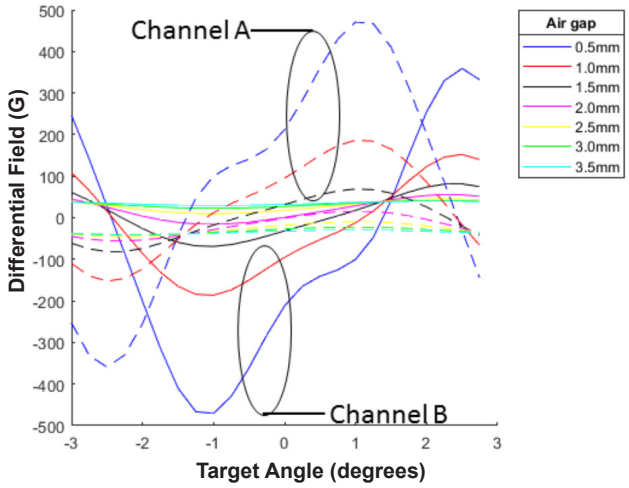

Figure 3: An example of the simulated differential channels of a sensor over one tooth-valley period of target rotation for the Allegro 60-0 target shown in Table 1. The dotted lines are channel A and the solid lines are channel B. Each channel is plotted at 7 different air gaps.

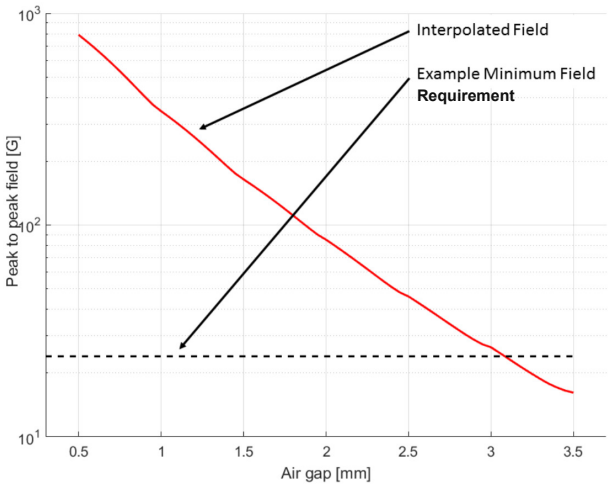

Figure 4: An example plot of peak-to-peak field vs. air gap. The maximum air gap is determined as the point where the interpolated field is equal to the minimum field. For back-biased sensors, the Allegro datasheet references the maximum air gap in mm with the Allegro Reference Target 60-0. Based on simulations or measurements, Allegro can determine the maximum air gap, across all boundary conditions identified in the datasheet, for bespoke target shapes. Contact an Allegro representative for support in evaluating the expected maximum air gap for a specific target design. Note that the y-axis uses a logarithmic scale.

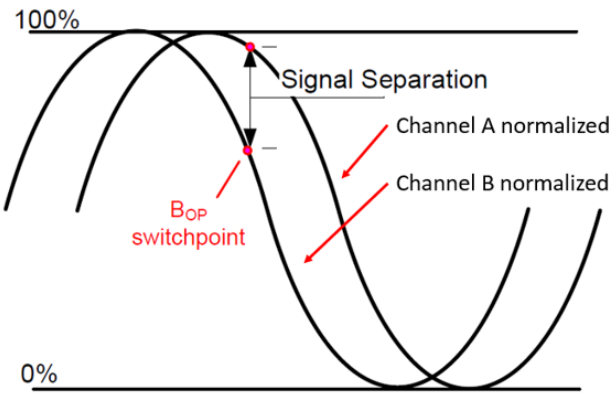

Figure 5: Definition of switch point separation

The data shown in the following sections is calculated for a worst-case temperature of 150°C, and the maximum air gap values are presented as a percentage of the maximum air gap measured for this particular sensor for this set of simulations. The trends shown in this report should be helpful for guiding steel target design. For more detailed application support and target-specific simulations, contact an Allegro sales representative.

MILLED TARGETS

The data presented here is from magnetic simulations, performed with the system shown in Table 1 and Figure 6.

The outer diameter of the target was held constant at 120 mm for all simulations in this section, since past analyses have shown that target diameter is not (independently) a major factor.

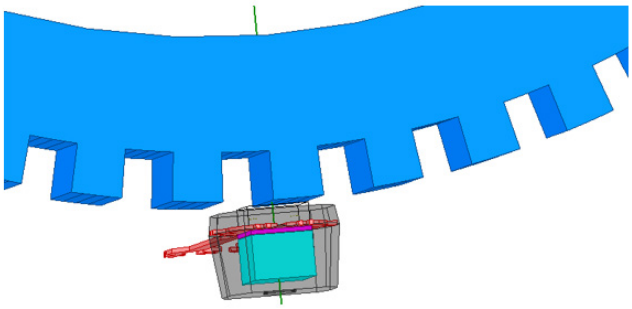

Figure 6: An example image from the simulation software Ansys Maxwell. The steel target is blue, the magnet is turquoise, and the concentrator is violet.

ASSESSMENT 1 – TOOTH LENGTH AND VALLEY WIDTH

For optimum device performance, it is vital to match the dimensions of the teeth and valleys on the target with the spacing of the Hall elements d_{Hall} in the sensor. As a first approximation, a target pitch T_{Cycle} (Valley width + Tooth length) of

$$T_{Cycle} = 4 \times d_{Hall}$$

is recommended, which should then be further optimized as discussed in subsequent sections.

One of the most important parameters for target design is the valley width—typically the maximum air gap is higher when the spacing between teeth is larger. The normalized maximum air gaps for three different sensors as a function of the tooth length and valley width, which are defined as distances along the circumference of a 120 mm outer diameter target, are shown in Figure 7. The maximum air gap is much more strongly affected by increasing the valley width than by increasing the tooth length.

Note that the points marked with X's have a switch point separation below 20%, and thus would result in unreliable direction detection and performance outside datasheet specification for the evaluated ICs. For both sensors, it appears that a tooth length greater than 4 mm results in unacceptable switch point separation. Increasing the valley width greatly improves the maximum air gap up to a valley width of approximately 8 mm, above which the performance reaches a plateau.

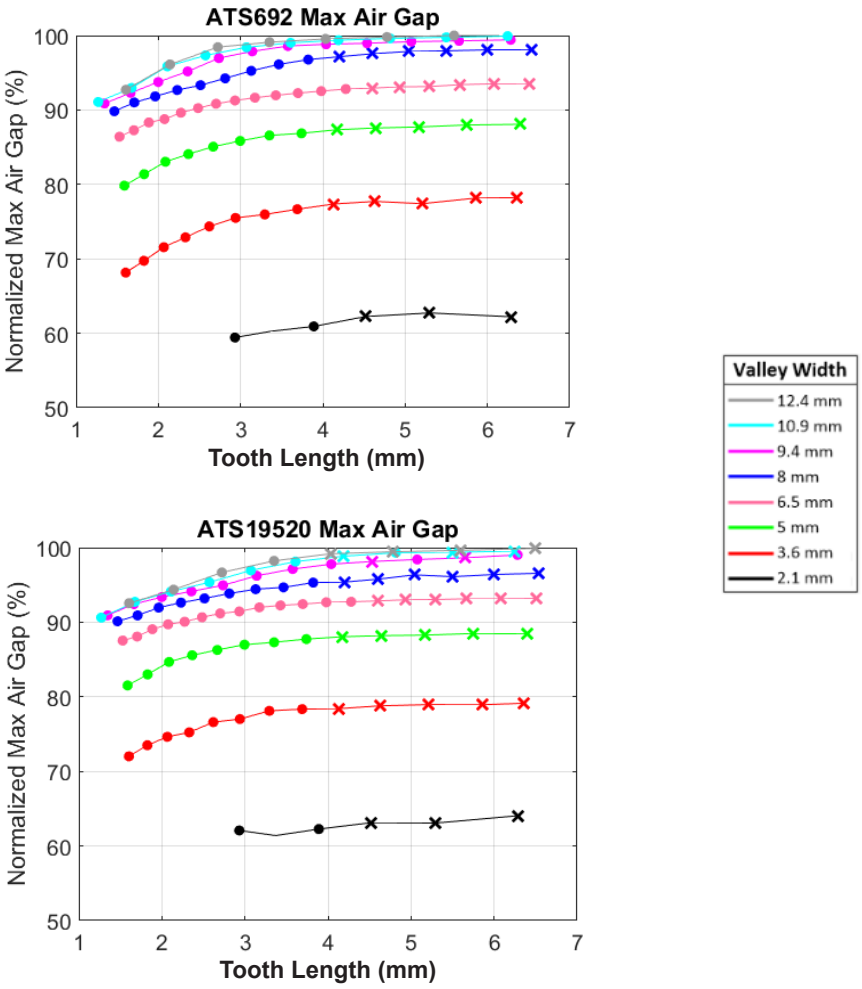

Figure 7: Maximum air gap as a function of tooth length aand valley width for three different Allegro back-biased sensors for a target with an outer diameter of 120 mm.

ASSESSMENT 2 – TOOTH SHAPE

Figure 8 and Figure 9 show examples of targets with varied tooth shape, retaining a constant valley width as measured at the root diameter, while changing angle of the tooth flank. Simulated maximum air gap is shown in Figure 10. The tooth angle here is defined relative to the target radius. For relatively small teeth and valleys, in this case 3.1 mm each, simulations show that increasing this angle initially improves maximum air gap performance up to an optimum angle of 10˚. This improvement can be understood to result from the increased space between teeth and is roughly equivalent to decreasing the tooth/valley ratio (see section above).

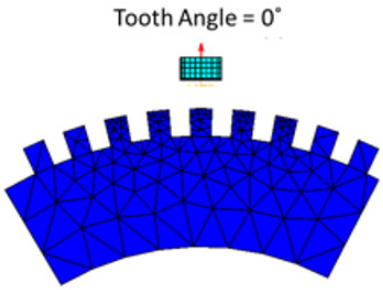

Figure 8: Example image of ferromagnetic target (blue) meshed for simulation with a tooth angle of 0°.

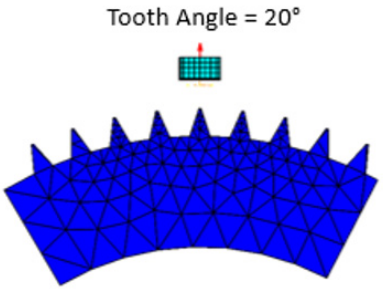

Figure 9: Example image of ferromagnetic target (blue) meshed for simulation with a tooth angle of 20° while retaining root valley width shown in Figure 8.

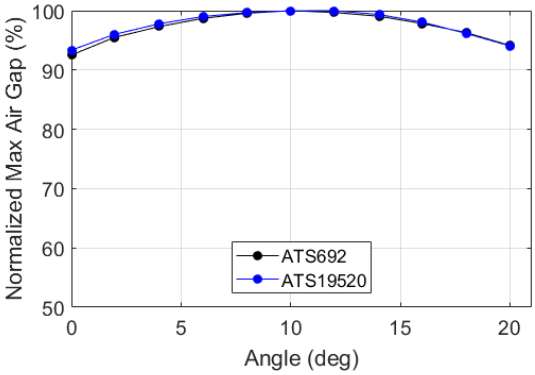

Figure 10: Normalized maximum air gap as a function of tooth angle starting from the nominal condition (OD = 120 mm, 3.1 mm tooth, 3.1 mm valley, 4 mm tooth height) and decreasing the circular tooth length in order to increase the tooth angle.

Thus, simulating the same set of tooth angles but with a larger valley width, as shown in Figure 11 and Figure 12, results in a different trend (Figure 13), with the maximum air gap falling monotonically as the tooth angle is increased.

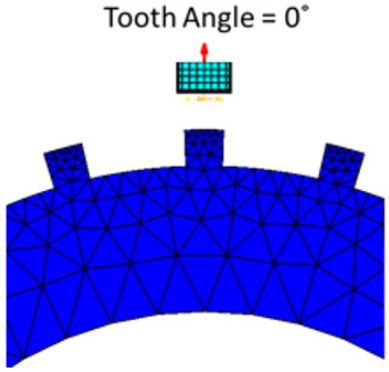

Figure 11: Example image of ferromagnetic target (blue) meshed for simulation with a tooth angle of 0°.

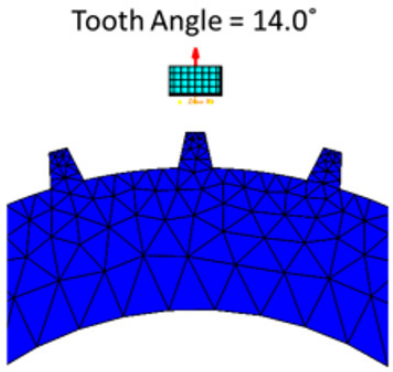

Figure 12: Example image of ferromagnetic target (blue) meshed for simulation with a tooth angle of 14° while retaining root valley width shown in Figure 11.

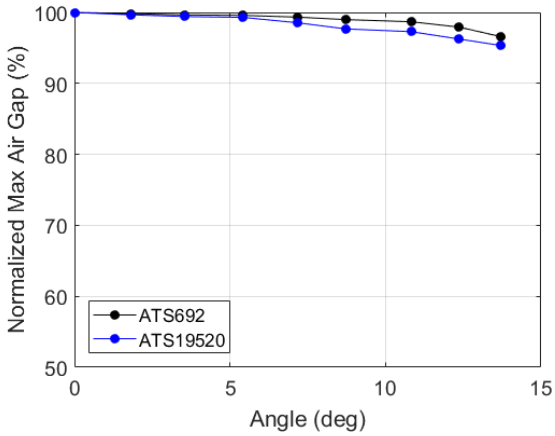

Figure 13: Normalized maximum air gap as a function of tooth angle starting from OD = 120 mm, 4.2 mm tooth, 11.5 mm valley and decreasing the circular tooth length in order to increase the tooth angle.

Alternatively, the tooth angle can be varied by keeping the circular tooth length constant and reducing circular valley width, as shown below in Figure 14 and Figure 15. In this case, there is a weak, monotonic reduction in the maximum air gap. This effect is like the reduction in maximum air gap when the valley width is decreased (see section above). This effect has a weak impact; however, it is recommended to use targets with a tooth angle near zero in this case.

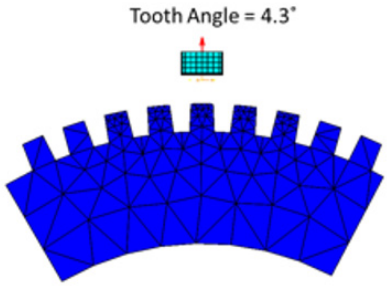

Figure 14: Example images of ferromagnetic targets (blue) meshed for simulation with a tooth angle of 4.3° while keeping circular tooth length constant.

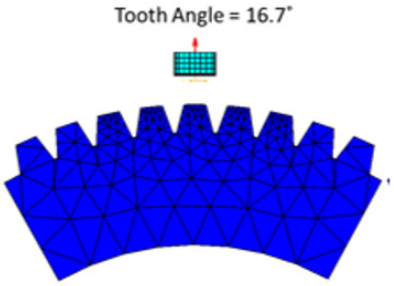

Figure 15: Example images of ferromagnetic targets (blue) meshed for simulation with a tooth angle of 16.7° while keeping circular tooth length constant.

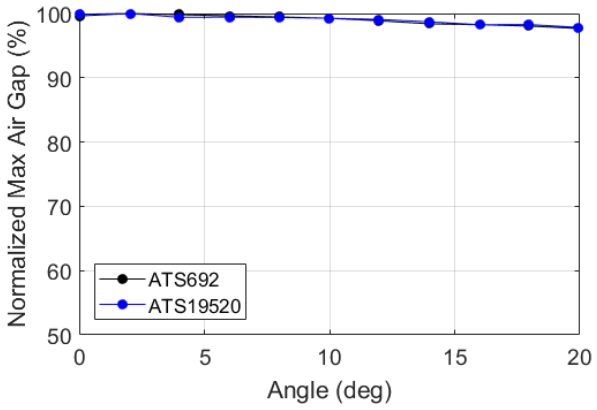

Figure 16: Normalized maximum air gap as a function of tooth shape starting from the nominal condition (OD = 120 mm, 3.1 mm tooth length, 3.1 mm valley width) and reducing the root valley width in order to increase the tooth angle.

ASSESSMENT 3 – TOOTH HEIGHT

As the differential magnetic signals measured by the Hall elements in the sensor are generated by modulation of the magnetic field of the integrated permanent magnet, the amount of material in front of the sensor has a significant impact on its performance. Modifying the tooth height of the target effectively varies the relative air gap changes between teeth and valleys. As shown in Figure 18, the normalized maximum air gap reaches a plateau where no further improvement can typically be achieved by increasing tooth height. The tooth height at which the plateau is reached depends on the tooth width and valley width of the teeth. In general, a tooth height of 4 mm or larger is recommended. When working with small feature targets (t <4.2 mm), a tooth height of 3 mm or larger may be appropriate as well.

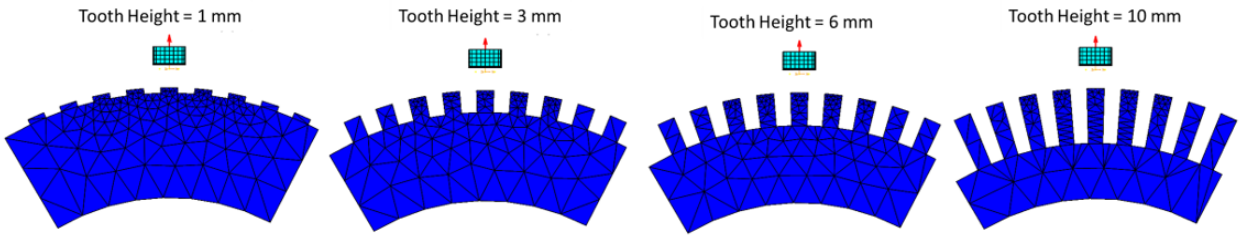

Figure 17: Example images of ferromagnetic targets (blue) meshed for simulation with varying tooth height.

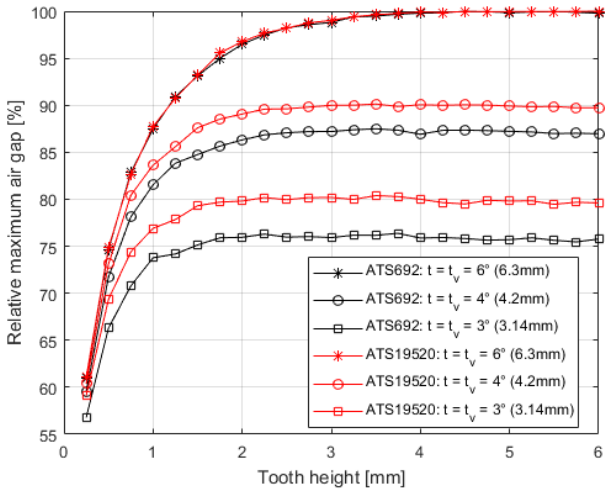

Figure 18: Normalized maximum air gap as a function of tooth height with constant OD = 120 mm and various tooth widths. Note that tooth width and valley width are assumed to be equal.

ASSESSMENT 4 – TARGET THICKNESS

When the thickness of the ferromagnetic target drops below the thickness of the back-bias magnet (in the vertical direction in Figure 19 below), maximum air gap starts to be affected. For example, the thickness of the magnet used for the ATS19520 is 3.8 mm, while for the ATS692 the magnet is 3.6 mm thick. For all sensors (see Figure 20), increasing the target thickness above approximately 4 mm has no effect on the maximum air gap, while decreasing the target thickness below 4 mm starts to have a significant negative impact. The above conclusions assume that the sensor is mounted perfectly central over the target. When designing the target for an application, manufacturing related placement tolerances should be considered as well. It is recommended to maintain a worst-case distance between the center of the sensor and the edge of the target of no less than 2 mm to avoid negatively impacting the maximum air gap capability.

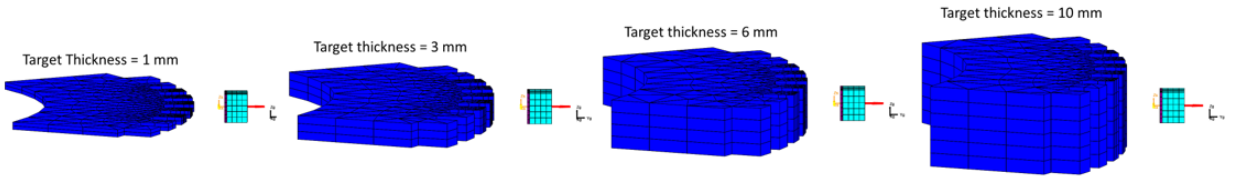

Figure 19: Example images of ferromagnetic targets (blue) meshed for simulation with varying target thickness.

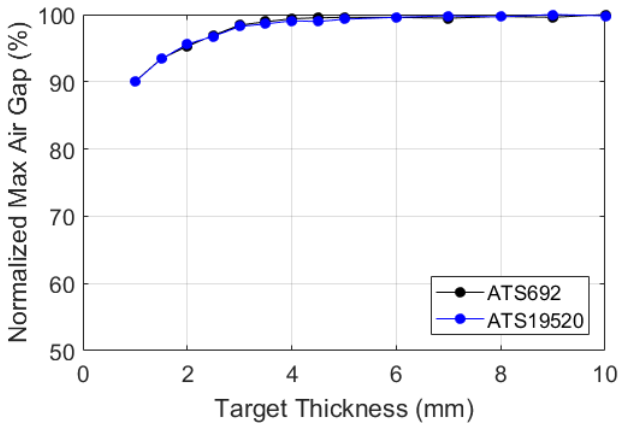

Figure 20: Normalized maximum air gap as a function of target thickness at the nominal condition (OD = 120 mm, 3° tooth-length, 3° valley-length).

STAMPED TARGETS

This type of target is typically produced by stamping holes into a sheet of metal. The holes can be interpreted as valleys of infinite depth and the areas between the holes as teeth resulting in a magnetic system comparable to milled targets. The data presented here are from magnetic simulations, performed with the system shown in Figure 23. In applications using this type of target, it is common to have ferromagnetic material, either from another rotating disc or a fixed piece of the assembly located behind the rotating target. Note that having such an adjacent ferromagnetic material is similar to a valley in the target of Figure 1. An example of such an assembly is shown in Figure 21 and Figure 22. The diameter of the target was held constant for all simulations in this application note, since the target diameter is not (independently) a significant factor.

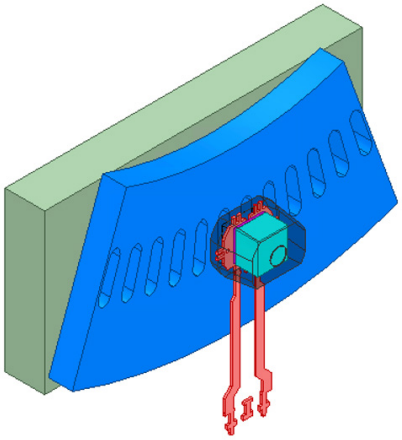

Figure 21: An example image from the simulation software Ansys Maxwell. The steel target is blue, the magnet is turquoise, and the lead frame is red. Shown in olive is a ferromagnetic plate situated behind the target.

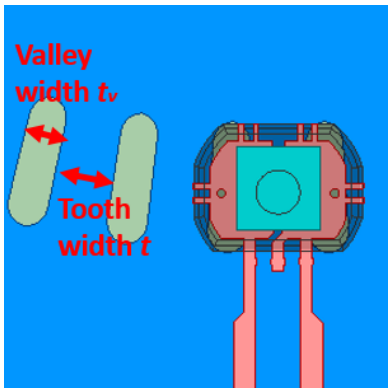

Figure 22: Definition of valley width and tooth width

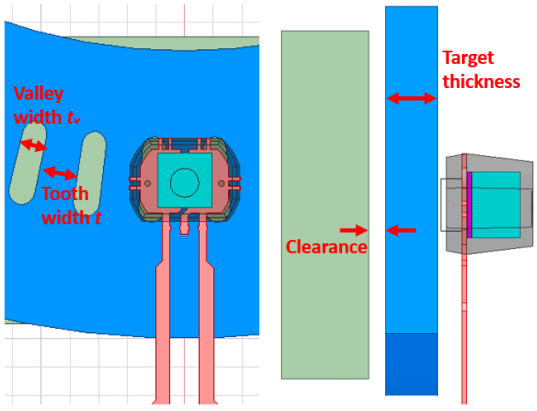

Figure 23: Definition of target thickness and valley clearance

ASSESSMENT 1 – ARC LENGTH (TOOTH AND VALLEY WIDTH)

A critical design parameter is the dimensioning of the stamped holes used in the target. Large tooth widths typically increase the maximum air gap, with no additional effect above 3.5 mm tooth width. For teeth with a tooth width smaller than 3.5 mm, the valley width becomes the dominating factor for maximum air gap capability, plateauing for valley widths larger than 6 mm.

Tooth widths of around 3 mm to 3.5 mm and valley widths larger than 6 mm allow for target designs without too much impact of small changes to either parameter.

Table 4: Normalized maximum air gap vs. tooth width and valley width.

Tooth Width [mm]	Valley Width [mm]	Maximum Air Gap Normalized [%]	
		ATS692	ATS19520
1.75	4.5	79	85
2.1	4	72	80
2.6	3.8	70	80
1.75 to 3.5	> 6	95-100	
> 3.5	> 3		

ASSESSMENT 2 – CLEARANCE

For small-feature targets—in this case both tooth and valley widths used were 2.6 mm—the depth of the valley, typically caused by a fixed or rotating plate mounted behind the target, does not have a significant influence on the maximum air gap, assuming a thickness of the stamped target of 3 mm and larger, as shown in Figure 24. For thicknesses smaller than 3 mm, an impact on maximum air gap is expected, as discussed in the next section. Comparing this to the tooth height for milled targets discussed in earlier sections, a stamped target with a thickness of 3 mm and a tooth height of 2 mm is approximately equivalent to a milled target with a tooth height of 5 mm. An impact on maximum air gap is expected once the sum of tooth height and target thickness drop below 4 mm.

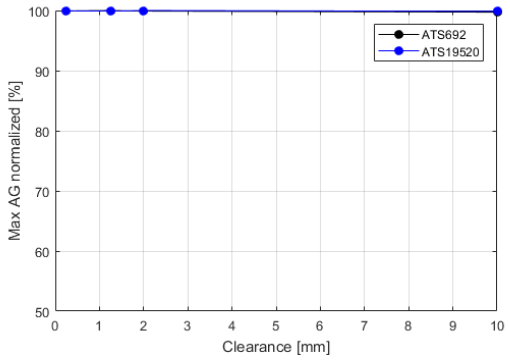

Figure 24: Normalized maximum air gap vs. clearance for a target thickness of 3 mm, a valley width of 2.6 mm and a tooth width of 2.6 mm.

ASSESSMENT 3 – TARGET THICKNESS

The thickness of the ferromagnetic material used as base material for stamped targets has an impact on device performance in cases where very thin materials are used. When choosing a target thickness of more than 1.5 mm, no significant impact on the maximum air gap is expected. However, thin targets typically are more prone to effects such as warping and run-out which can result in a change of air gap between sensor and target for different positions on the target. This can negatively impact the performance of the sensors with this particular target; therefore, the thickness of the target should be carefully chosen as to avoid such effects.

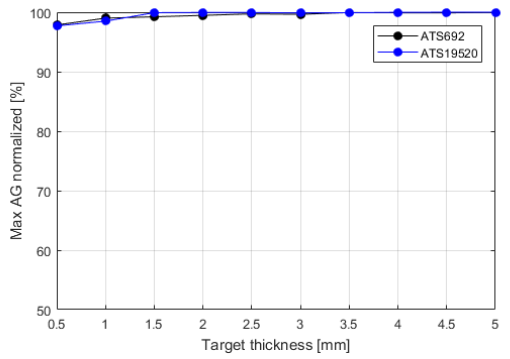

Figure 25: Normalized maximum air gap vs. target thickness.

CONCLUSIONS

This application note has detailed the impact of multiple target design parameters on the maximum air gap achievable with Allegro's ATS692LSH and ATS19520LSN transmission sensors, allowing for measurement of speed and direction of rotating targets. Two types of targets, representing the majority of targets used in today's transmission applications, namely milled and stamped targets, have been analyzed. In following the recommendations in this application note, target design decisions can be supported. Prior to the start of production tooling, it is highly recommended to perform in-application verification testing. For further support in evaluating the performance of Allegro's sensor components with specific targets, especially for applications requiring high performance or large air gaps, contact your local Allegro sales representative.

The conclusions drawn throughout the document are qualitatively applicable to other Allegro back-biased sensors of the same Hall-element spacing and sensor package, the latter defining the integrated permanent magnet.

Revision History

Number	Date	Description	Responsibility
–	November 2, 2020	Initial release	E. Burdette

955 PERIMETER ROAD • MANCHESTER, NH 03103 • USA
+1-603-626-2300 • FAX: +1-603-641-5336 • ALLEGROMICRO.COM